7th US National Combustion Meeting
of the Combustion Institute
Hosted by the Georgia Institute of Technology, Atlanta, GA
March 20-23, 2011

# Fundamentally Based Reaction Mechanism for Oxidation of Isooctane

*R. Asatryan,[1] S. Raman,[2] P. A. Bielenberg,[2] B. Peterson,[2]*
*J. W. Bozzelli,[1] and W. Weissman[2]*

*[1]Department of Chemistry and Environmental Science, New Jersey Institute of Technology, Newark, NJ 07102, USA*

*[2]ExxonMobil Research and Engineering Co., 1545 Rt.22 East, Annandale, NJ 08801, USA*

Isooctane is a component of Primary Reference Fuel and elementary mechanisms for its oxidation have been studied extensively, although a detailed analysis of its thermochemistry and oxidation kinetics by high-level quantum chemical methods has been limited by its complex structure and large size. Reduced reactivity of isooctane at low-temperature and its resistance to ignition, as opposed to linear alkanes, are generally attributed to its high degree of branching. Current kinetic models are mainly based on empirical rules, bond enthalpies and generic rate parameters, yet branched semi-rigid structural features of isooctane introduce specific reaction channels that are either irrelevant or non-feasible in smaller model systems. This report, to the best of our knowledge, is the first fundamentally based study of relevant pathways on the potential energy surfaces of all possible (1°/2°/3°) octyl radicals+$O_2$ using DFT and higher composite level calculations. We have particularly focused on the lowest energy reaction channels, which include dissociative ring-closure in intermediate hydroperoxy-octyl radicals and OH-transfer reactions back to the alkyl-radical centers. The last class of reactions, with a variety of significant product formation pathways, is very new for this intricate reaction system and is completely missing in all other kinetic models. The further chemical activation of intermediate hydroperoxy-octyl radicals (second $O_2$-association) leading to chain-branching is considered in detail and results are compared to the linear systems to establish its kinetic significance.

## 1. Introduction

Isooctane (2,2,4-trimethylpentane, neopentylpropane) is one of 18 isomers of octane found in gasoline, diesel and jet fuel [1-3]. It is a component of primary reference fuel (PRF) and defines the 100 point on the octane rating scale. The pure *n*-heptane component defines the zero point while mixtures of isooctane and *n*-heptane are used to define the range between the two extremes. Isooctane is the basic model of branched alkanes and its oxidation has been studied extensively using diverse experimental techniques and kinetic models [4-10]. Early kinetic mechanisms have primarily focused on simplified models, physical and chemical properties. With the advances in automated mechanism generation, current kinetic models incorporate a more comprehensive reaction network accounting for most of the reaction classes in combustion chemistry. However, the kinetic parameters are based on estimation procedures and are derived from simple model systems that often do not represent the complexity of isooctane structure. Herein, we investigate the detailed potential energy surface of radicals of isooctane with $O_2$ to

better understand the kinetics of structurally strained isooctane system and the efficiency of estimation procedures.

Branched alkanes (isooctane) are known to be less reactive in low temperatures typical of end-gases in spark-ignited engines in contrast to highly reactive straight alkanes (*n*-heptane). Isooctane has negligible reactivity at relatively low pressures where *n*-heptane undergoes low temperature oxidation and higher pressures are necessary to induce low-temperature oxidation in isooctane where *n*-heptane undergoes high-temperature ignition [6]. It is generally believed that the branched structure of isooctane reduces its reactivity at low temperatures explaining its resistance to autoignition as opposed to linear alkanes. Isooctane with its branched structure, however, is expected to introduce channels that are either irrelevant or not feasible in smaller or linear fuel components.

Antiknock efforts in particular are aimed to inhibit the low-temperature pre-flame chain branching chemistry of peroxy radicals by increasing the amount of branching in the hydrocarbon component. Furthermore, all types of catalytic upgrades to increase octane number of gasoline are directed to form *iso*- and branched paraffins via alkylation, reforming and isomerization processes [2]. Therefore, it is of importance to understand the detailed chemistry of isooctane combustion and the effect of branching to improve the kinetic models for more accurate predictions of engine performance and pollutant formation.

Experimentally, ignition and specie profiles in isooctane combustion are studied extensively using shock tubes, rapid compression machines (RCMs), flames, jet stirred reactors, and flow reactors (see, e.g., a recent study [4] and references cited therein). Direct measurements of intermediates of ignition are challenging experimental objectives, yet such measurements are critical for the understanding of fuel decomposition and oxidation pathways. Wooldridge *et al.*[5] published detailed product analysis in the rapid compression facility studies of isooctane ignition and quantified 30 hydrocarbons and oxygenate species. The results are compared with the model predictions of detailed reaction mechanism developed by Curran et al. [10]. *Iso*-butene (i-$C_4H_8$) and propene ($C_3H_6$) were the major olefin species identified in these experiments. Chen et al [8] have identified and quantified twenty-three hydrocarbons and oxygenated intermediate species as a function of time at pressures of 6 and 9 atm while studying diluted stoichiometric oxidation of isooctane in the intermediate temperature range. These experimental results were also modeled using Curran's detailed mechanism. Notably, they found significant differences in the predictions of the mole fractions of two important products, *viz.,* the most abundant *acetone* and methacrolein products, the formation of which is assigned to the products of *iso*-butene oxidation. As presented below, there are direct channels for the formation of these key products which are missing in current detailed mechanisms.

In contrast to the low-temperature combustion of normal HC, which are known to produce mainly simple ketones and aldehydes, oxidation of branched isooctane fuel component is primarily characterized with the formation of carbo- and heterocyclic systems [5-8]. For both reference fuel hydrocarbons (*n*-heptane and isooctane), tetrahydrofurans are the major O-heterocycles formed in cool flames. The main products from low-T oxidation of isooctane are formaldehyde, $CH_3CHO$, *acetone* (2-propanone) and dimethylpropionaldehyde $(CH_3)_3CCHO$. Among cyclic ethers *2,2,4,4-tetramethyl-tetrahydrofurane* (2,2,4,4-TM-THF) is the most abundant one. Olefinic hydrocarbons comprise iC8-conjugate olefins, iso-butylene, some iC7-olefins and trace amounts of ethylene and propene [6]. In comparison, the products from *n*-

heptane low-T combustion include mainly $CH_2O$, acetic-, propion- and butyraldehydes. Cyclic ethers $C_7H_{14}O$ comprise of 10 mol %, mainly 2-Me-5-Et-THF [6].

The formation of cyclic ethers in combustion of liquid hydrocarbons has been known from late 1950s [11]. Radical center attacks the peroxy linkage leading to the dissociative ring-closure. This cyclization is accompanied by the elimination of OH-radicals and the mechanism of this reaction step has been analyzed rather extensively by Chan *et al.* [12] and Wijaya *et al.* [13].

Intramolecular radical attack of proximal O-atom of peroxy group is alternatively shown to initiate formation of intermediate hydroxyl-alkoxy type radicals in combustion of hydrocarbons [14] and oxidation of sulfur-containing compounds [15]. This mechanism appears to be very intriguing especially for isooctane with semi-rigid "rich" structural features (*vide infra*). Specified cyclization and OH-transfer reactions basically are two lowest energy pathways in oxidation of isooctane comprehensively addressed in this study.

Earlier [17], we briefly reviewed several kinetic models for isooctane oxidation starting from the earliest global Shell model and including the more advanced models based on automatic reaction mechanism generation software such as EXGAS counting extensive reaction sets [9]. We find the detailed kinetic model of Curran et al. [10] to be the more often used mechanism for modeling of isooctane combustion. The kinetic parameters in this mechanism are largely based on group additivity estimates and the mechanism includes 857 species and 3606 reactions. However, even in its latest edition (updated PRF-model of NUI/LLNL [16]) contains some inconsistent kinetic parameters. Unfortunately, any adjustment of kinetic parameters unavoidably leads to the significant variation of initial input data.

Existing literature thus highlights the necessity of first principle based systematic investigation to improve our understanding of branching on the oxidation mechanism. Based on this, we studied in detail the PES of oxidation reactions of *all possible* isooctyl radicals using DFT and higher level composite methods. To the best of our knowledge, this is the first attempt to describe fundamentally oxidation of a hydrocarbon as large as isooctane ($i$$C_8H_{18}$). The present work is focused on the analysis of oxygenation reactions of isooctyl radicals which include: chemical activation, association, insertion, unimolecular dissociation, and elimination reactions.

Chemically activated peroxy radicals may isomerize to other species, dissociate back to reactants, or transform to products through various ($P$,$T$)-dependent channels [19]. These channels involve large number of wells to products and metastable intermediates, many of which are important under varying conditions. For isooctane and most alkane oxidation reaction systems, there exists a competition between pathways with higher pre-exponential factors such as direct elimination reactions, which would dominate at higher temperatures and low-energy barrier elimination reactions feasible at low-temperatures. Main focus of this work is low-temperature processes involving first-step activation processes, yet, principal calculations are performed for much more complex and intriguing (*cf.* detailed PES for 2-pentyl+$2O_2$ [18]) second oxygenation reactions of isooctyl radicals.

## 2. Computational Methodology

Potential energy surface (PES) for dual oxidation reactions of isooctane peroxy radicals ($C_8H_{17}$•+$O_2$ and subsequent $C_8H_{17}O_2$•+$O_2$) are calculated using B3LYP hybrid density functional theory (DFT) [20] in conjunction with the moderate size 6-31G(d) basis set, as implemented in

Gaussian 03 suite of programs [21]. This is the relatively low cost computational tool well recommended in analyzing the structure of PES stationary points (location of TS and minima) in oxidation of extended systems [15,18,19,22]. The relative energies have been verified at higher CBS-QB3 level, which includes more refined CCSD(T) level calculations, empirical terms and corrections for spin contamination in corresponding calculation schemes to predict molecular energies to around 1 kcal $mol^{-1}$ accuracy [23].

The CBS-QB3 method has an advantage of utilizing geometry and frequencies calculated at the same level of theory, *viz.* B3LYP/6-311G(2d,d,p), which is important for correct localization of TS structures along with other benefits of the CBS-QB3 method such as extrapolation of energetics to the complete basis set limit and inclusion of higher levels of correlation [18].

We also employed the G3MP2B3 multilevel method and a variety of other DFT functionals and basis sets to select a reasonable and computationally cost effective method. However, due to the space limitation we do not include the methodological details and the comparative performance at different levels in this publication; they will be published in the forthcoming elaborate version of the current article [17].

Transition states are characterized as having only one negative eigenvalue of Hessian (force constant) matrices. The absence of imaginary frequencies verifies that structures are true minima at their respective levels of theory. Intrinsic reaction coordinate (IRC) calculations were performed at B3LYP/6-31G(d) level to ensure connectivity of stationary points. In addition, the final point geometries at both sides of TS were re-optimized to proper minima.

***Species Notation:*** A new notation system is developed in our previous work on oxidation of *n*-pentane [18]. This is a general and short notation that simplifies the book-keeping of similar reaction schemes of homologous hydrocarbons in detailed kinetic models as opposed to commonly employed numbers or non-descriptive (non-perceptive) symbols.

Abbreviated names are employed for larger products and reagents. Isooctane derived species are presented as IO-AJ, IO-CQJ, IO-CQAJ for radicals (*vide infra*), where IO represents isooctane, Q stands for an OOH group and J is a radical center. A, B, C and D indicate the skeletal position of carbon atoms while specific symbols and letters describe attached substituent or hybridization, *e.g.,* QJ for a peroxy radical group, * for a double bond, # for a triple bond, and M for a methyl group, etc.

Four distinct positions are highlighted in Figure 1. There are nine primary-A, six primary-D, two secondary-B and only one tertiary-D type hydrogen atoms. Using new notations for instance, one can express radicals on A-position as IO-AJ. Hydroperoxy radical on the B-position would be IO-BQJ, and the bulky $(CH_3)_2(CH_2OOH)CCH(OO\bullet)CH(CH_3)_2$ intermediate radical maybe abbreviated as IO-AQBQJ, etc.

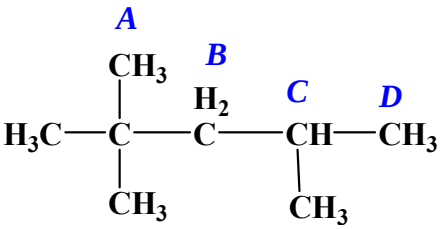


**Figure 1. Definition of skeletal atoms in isooctane molecule**

Primary hydrogen atoms prevail, yet the tertiary C-H bond has a substantially lower dissociation enthalpy. BDE for primary (A, D), secondary (B) and tertiary (C) C-H bonds as computed at the CBS-QB3 level are 101.0, 100.9, 97.2 and 94.1 kcal $mol^{-1}$, respectively. At low to mid combustion temperatures preceding to IC engine ignition, the tertiary bond is expected to be cleaved first, to form the IO-CJ alkyl radical, which associates further with $O_2$ and generates IO-CQJ activated peroxy adduct. The peroxy radical center being located in the middle of molecule has easy access to all other H-atoms to isomerize to hydroperoxy-alkyl radical intermediates *via* less strained 7-and 5-membered ring TS.

For this reason, the potential surface for oxygenation (chemical activation) reactions of IO-CQJ tertiary peroxy radical of isooctane is studied in more detail (Figs.2-4) and justification of our calculation methods is verified through the re-calculation of key stationary points with higher level methods, on this IO-CQJ +$O_2$ PES.

The formation of primary A- and D-carbon radicals is expected to be more important at higher temperatures due to the larger dissociation energy of primary C-H bonds where reverse decomposition of $RO_2$ is more competitive. For the primary IO-AQJ, IO-DQJ and secondary IO-BQJ peroxy radicals, we focus more on the two most relevant, competitive, low energy pathways *viz.,* dissociative ring closure versus intramolecular OH migration.

## 3. Results and Discussion

***Isomerization of Peroxy Radicals:*** Intramolecular isomerization in peroxy radicals is the most important step in oxidation of hydrocarbons at low temperatures. Intramolecular propagation via H-migration in small $RO_2$• and •OOR'OOH (second oxygenation adduct) radicals are systematically studied and general trends are well established ([22,24,26-28], and references therein). In this regard, here we address briefly some specific aspects of the isomerization of isooctyl radicals.

Figures 2a and 2b show typical isomerization processes involving the primary A-peroxy radical *via* abstraction of tertiary C-position hydrogen atom (7-member ring TS-C1A), and abstraction of an A-hydrogen atom by C-peroxy radical intermediate *via* the TS-A1C, respectively.

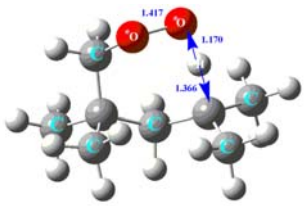


a) TS-C1A

b) TS-A1C

TS-A1C

**Figure 2. (a) Lowest energy isomerization of IO-AQJ iso-octyl peroxy radical to IO-AQCJ hydroperoxy radical; (b) TS for H-transfer (isomerization) from a primary A-position to tertiary peroxy center IO-CQJ forming IO-CQAJ. Transition vectors are sketched.**

Abstraction of the tertiary hydrogen atom by peroxy group located at A-position, *viz.,* IO-AQJ → IO-AQCJ is the lowest energy process among the H-transfer reactions involving any isooctane peroxy radicals. The activation barrier $\Delta H^{\#}$ (TS-C1A) is as low as *ca.*17 kcal $mol^{-1}$ (16.74, 17.09, 16.95 kcal $mol^{-1}$, correspondingly, at B3LYP/6-31G(d), G3MP2B3, and CBS-QB3 levels of theory in agreement with the unified parameter of 17.05 kcal $mol^{-1}$ used by Curran et al. for all 7-

memberred ring TS transitions [10]). This value is lower by 7-15 kcal $mol^{-1}$ than those for other isomerization reactions. Importantly, the difference between two predicted values at B3LYP/6-31G(d) single level DFT and the G3MP2B3 composite method employing the same level of geometry calculation, is only 0.35 kcal $mol^{-1}$. In this case it is an exceptionally good agreement. This is also consonant with literature data (comparative analysis of all relevant H-transfer processes will be presented elsewhere [17]).

It should be highlighted that the easiest to form IO-CQJ peroxy radical has no options involving 6-membered ring TS to isomerize, where six membered ring H atom transfer is commonly believed to be the kinetically most suitable isomerization channel for linear hydrocarbons. TS-A1C (Fig.2b) included also in PE diagram in Fig.3, deals with a 7-membered TS-ring and involves higher activation energy at 24.4 kcal mol-$^{1}$ due to endothermicity.

The barrier for a typical 6-membered ring TS isomerization of IO-BQJ → IO-BQAJ is calculated as 25.2, 23.2, 23.7 and 22.2 kcal $mol^{-1}$, correspondingly, at B3LYP/6-31G(d), B3LYP/6-31G(d,p), G3MP2B3 and CBS-QB3 levels of theory *vs.* the generalized 24.0 kcal $mol^{-1}$ estimate of Curran et al. [10]. In original version of Curran's mechanism [10], the value of 24.4 kcal $mol^{-1}$ was used, however in the recent update [16] it is somewhat reduced to 24.00 kcal $mol^{-1}$ which according to authors speeds up substantially second $O_2$-addition process and increases efficiency of chain-branching and OH + ketohydroperoxide formation.

The above calculated values show the barriers and reaction enthalpies for the IO-BQJ, intramolecular transfer of H-atoms (*cf.* TS-A1C in Fig.3) are somewhat overestimated at the B3LYP/6-31G(d) level. This is particularly due to the lack of *p*-polarization extension functions in the basis sets for hydrogen atoms, although the energies of other types TS dealing with heavy atoms, are in fairly good agreement with higher level results (*vide infra*).

Judging from benchmark calculations of Zheng and Truhlar [22], the B3LYP functional is of good performance in butoxyl radical reactions compared to CCSD(T)/CBS method including the core-valence correlation contributions and scalar relativistic corrections. From a wide variety of tabulated results in [22] one could extract that the stability of radicals with spin located on O-atoms is somewhat underestimated by B3LYP functional. This is in full agreement with the underprediction of well depths for association reaction $R\bullet+O_2 \rightarrow RO_2\bullet$ observed here.

***Well Depths:*** The only and consistently persistent exception in performance of B3LYP/6-31G(d) method is the (rather expected) underprediction of well depths, the reaction enthalpy of initial association reaction of alkyl radicals with oxygen. Consequently, well depths were evaluated additionally at higher computational levels employing either atomization [25] or work reaction procedures. The values calculated at CBS-QB3 level using a more complex isodesmic reaction scheme [17] is in close agreement with the value arrived from the direct dissociation limit for the reaction $RO_2 \rightarrow R+O_2$ (34.1 *vs.* 34.7 kcal $mol^{-1}$, respectively).

Another systematic (additive) error in B3LYP energetics can be traced to the overestimation of the enthalpy of $^3O_2$-molecule; this has been corrected with bond additivity corrections. In the PE-diagram shown in Fig.3, we show the non-corrected value in blue to be consistent with relative energies of other stationary point. Some remaining discrepancy is likely due to the under-estimation of dispersion interactions and electron correlation in B3LYP calculation scheme [17].

***Comprehensive PES for IO-CJ+$O_2$ Reaction System:*** As mentioned above, it is *a priori* expected that the initial reactions of IO-CJ+$O_2$ → intermediates, will have a dominant role in low temperature processes, especially at higher pressures. Association of an oxygen molecule with the only tertiary isooctyl radical forms a peroxy radical-adduct IO-CQJ (*via* TS-A1C, Fig.3).

Further isomerization of this peroxy radical occurs *via* 5 and 7 membered ring transition states, correspondingly to form IO-CQBJ and IO-CQDJ hydroperoxy radicals via abstraction of B secondary and D primary hydrogen atoms, as well as a IO-CQAJ radical *via* the transfer of any one of the nine A-primary hydrogen atoms to C-peroxy radical center (TS-A1C, Fig.2).

Fig.3 details a PE diagram for the formation and further transformations of the IO-CQAJ hydroperoxy alkyl intermediate. There are two additional isomerization processes (with further reaction steps) for the chemically activated IO-CQJ peroxy radical (from B and D positions) not presented here [17].

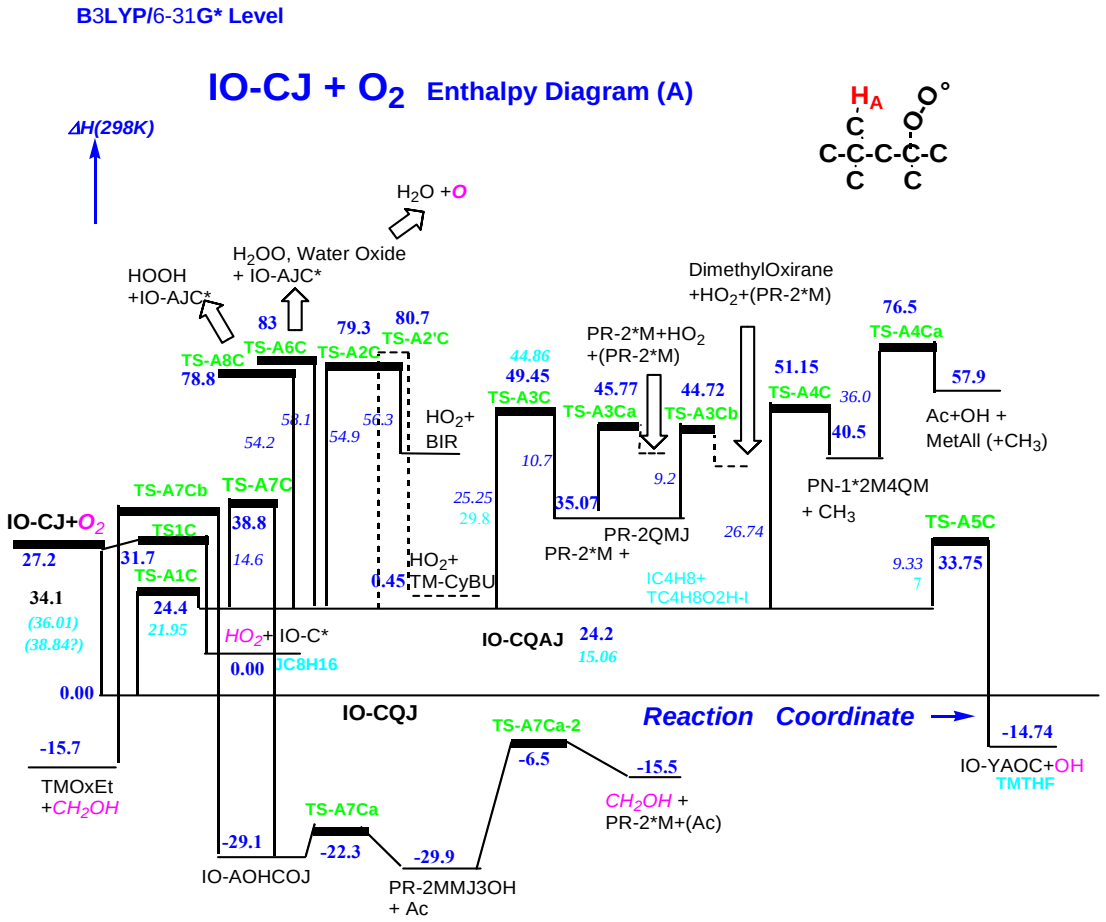


**Figure 3. Comprehensive enthalpy diagram for chemical activation reactions of IO-CQJ tertiary isooctyl-peroxy radical via abstraction of an A-primary hydrogen atom (IO-CJ+$O_2$ → IO-CQJ →IO-CQAJ → Products). Calculated values are in dark and literature estimates in light blue.**

Although the main set of reactions is considered to be known *a priori*, or from the lower homologues [8], some reaction schemes as one can see from Fig. 3, are missing from current schemes. There are in addition, uncertainties and arbitrary estimates in the parameters for the complex association-transformation reactions. Further reactions of primary intermediates appear

to be more complex and less perceptive than it is assumed from the simple chemical intuition; and they lead to the generation of products observed in experiments that are not modeled.

We believe that some of the reaction schemes presented here are new reactions that occur only when such a large and branched hydrocarbon backbone is considered. Lowest energy pathways via TS-A5C and TS-A4C lead to the formation of the experimentally observed, most abundant cyclic ether 2,2,4,4-TM-THF and the 2-propanone (acetone)[6]. While cyclic ether formation is the low energy process, in full accordance with experiments, acetone formation requires higher barriers. This channel would underestimate acetone formation as it takes place in Curran's mechanism used by Wooldridge *et al.*[5] (*vide supra*). We explain excessive production of acetone by an alternative channel involving a low-energy OH-transfer pathway via TSA7C (Fig.4) and leading to the low-energy formation of •$CH_2OH$ radical together with other important products such as oxetane, acetone, and *iso*-butene. This is a new reaction pathway and is expected to contribute significantly to the low temperature reaction kinetics.

The PE-diagram (Fig.3) also illustrates several non-traditional reaction channels such as generation of atomic oxygen via the formation of $H_2O_2$ and water oxide, $H_2OO$ intermediates, which will be of importance in certain high-T or irradiated media.

Reaction mechanisms and typical TS structures for lowest energy dissociative ring-closure (TSA5C) and intramolecular OH-transfer (TSA7C) pathways for IO-CJAQ hydroperoxy radical are illustrated in Fig.4. These are the two competitive unimolecular decomposition channels that are in the detailed PES of IO-CQJ (Fig.3). A comparison of results for other, similar channels are presented below.

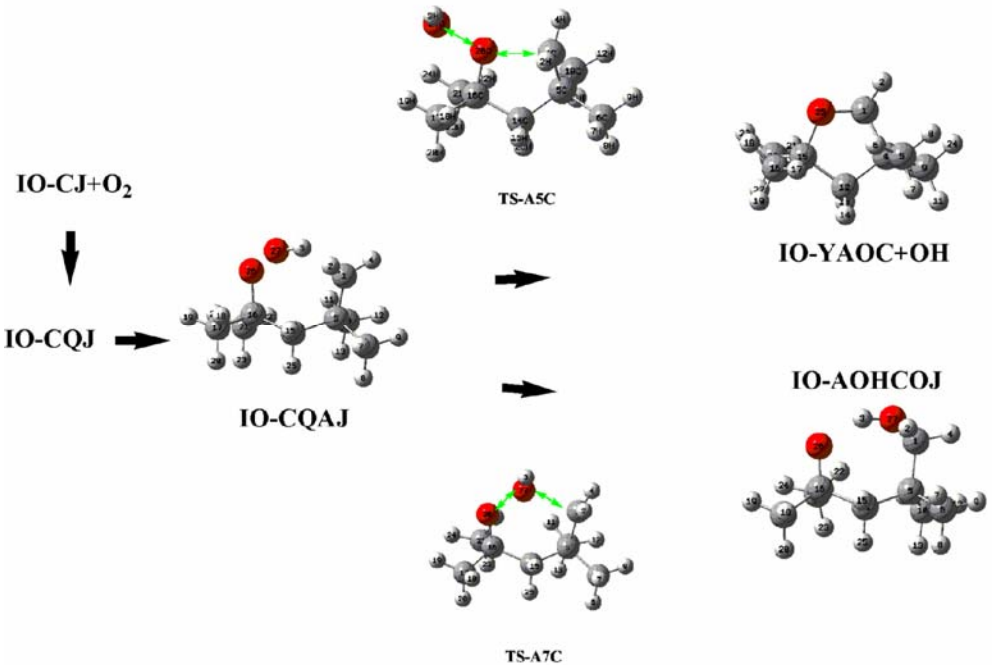


**Figure 4. Typical lowest energy reaction pathways: Ring-Closure via TS-A5C and OH-transfer via TS-A7C in IO-CQAJ hydroperoxy radical.**

***Cyclization and OH-Transfer Reactions:*** Computed DFT results are in good agreement with composite level calculation results for the two dominant pathways. Tables 1 and 2 summarize

the reaction barrier and heat of reaction for these two channels from all radicals considered in isooctane at the B3LYP level.

**Table 1. Formation of Hydroxyl-Alkoxy Radical Adducts via OH-Transfer Arranged by TS Ring-Size at B3LYP/6-31G(d) Level**

| Reagent [a] (TS-ring-size) | TS | Adduct [b] | $\Delta H^{\#,}$ kcal mol$^{-1}$ | $\Delta H_{rxn,}$ kcal mol$^{-1}$ | Decomposition Products [c] | $\Delta H^{\#,d}$ kcal mol$^{-1}$ |
|---|---|---|---|---|---|---|
| **IO-BQCJ** (4) | **TS-C7B** | **IO-BOJCOH** | 15.83 [e] | -68.74 | PR-2MM3J + PR-2OH3*O | 21.44 |
| **IO-CQBJ** (4) | **TS-B7C** | **IO-COJBOH** | 28.67 | -68.47 | PR-2*O + PR-2MM3OH | 21.99 |
| **IO-CQDJ** (4) | **TS-D7C** | **IO-COJDOH** | 24.92 | -50.19 | BU-2MM4J + PR-2*O3OH | 9.40 |
| **IO-DQCJ** (4) | **TS-C7D** | **IO-DOJCOH** | [f] | -42.65 | $CH_2O$ + PN-2MM4JOH | 1.93 |
| **IO-AQAJ** (5) | **TS-A7A** | **IO-AOJAOH** | 22.55 | -53.25 | $CH_2O$ + PN-2MOH4M | -0.82 |
| **IO-AQBJ** (5) | **TS-B7A** | **IO-AOJBOH** | 19.30 | -48.43 | $CH_2O$ + PN-2M4M3OH | 3.20 |
| **IO-BQAJ** (5) | **TS-A7B** | **IO-BOJAOH** | 19.88 | -73.50 | PR-2M3*O + PR-2JM3OH | 20.59 |
| **IO-BQDJ** (5) | **TS-D7B** | **IO-BOJDOH** | 21.39 | -71.92 | PR-2MM3J+PR-2MOH3*O | 22.55 |
| **IO-CQAJ** (5) | **TS-A7C** | **IO-COJAOH** | 14.65 | -53.50 | PR-2*O + PR-2MMJ3OH | 6.80 |
| **IO-DQBJ** (5) | **TS-B7D** | **IO-DOJBOH** | 22.72 | -48.63 | $CH_2O$ + PN-2MM3OH4J | 8.88 |
| **IO-DQDJ** (5) | **TS-D7D** | **IO-DOJDOH** | 19.37 | -52.65 | $CH_2O$ + PN-2MM4J5OH | 11.15 |
| **IO-AQCJ** (6) | **TS-C7A** | **IO-AOJCOH** | 12.12 | -49.70 | $CH_2O$ + PN-2JM4OH | 5.42 |
| **IO-AQDJ** (7) | **TS-D7A** | **IO-AOJDOH** | 7.06 | -52.33 | $CH_2O$ + PN-2JM5OH | 0.3 |
| **IO-DQAJ** (7) | **TS-A7D** | **IO-DOJAOH** [e] | [f] | -53.41 | $CH_2O$ + PN-2MMOH4J | 7.58 |

[a] Hydroperoxy-alkyl radicals, [b] Hydroxyl-alkoxy radicals, [c] In linear HCs we employed position numbers and substituent [18], e.g. PR-2*O stands for acetone and PR-2*M for iso-butene, or PN-2MM4J5OH for 2,2-dimethyl-5-hydroxy-4-pentyl radical, [d] Enthalpy of activation for adducts decomposition, [e] Elimination of $H_2O$, see text, [f] No converged TS is localized.

**Table 2. Formation of Oxocyclic Adducts Arranged by TS Ring-Size at B3LYP/6-31G(d) Level**

| Reagent [a] (TS-ring-size) | TS | Oxocycle [b] | $\Delta H^{\#,c}$ kcal mol$^{-1}$ | $\Delta H_{rxn,}$ [c] kcal mol$^{-1}$ | Literature, Estimates, Models |
|---|---|---|---|---|---|
| **IO-BQCJ** (3) | **TS-C5B** | **YCOB** | 5.62 | -32.25 | Wijaya *et al.* 13.4; 15.9; 17 [d] |
| **IO-CQBJ** (3) | **TS-B5C** | **YCOB** | 25.83 | -31.47 | Curran *et al*. 22 |
| **IO-CQDJ** (3) | **TS-D5C** | **YCOD** | 8.64 | -33.25 | Buda *et al.* 17.95 (16.5) |
| **IO-DQCJ** (3) | **TS-C5D** | **YCOD** | 10.08 | -10.88 | Chan *et al.* 13.8 |
| **IO-AQAJ** (4) | **TS-A5A** | **YAOA** | 14.73 | -17.80 | Wijaya *et al.* 17.4; 19.5; 21.9[d] |
| **IO-AQBJ** (4) | **TS-B5A** | **YBOA** | 11.70 | -20.38 | Chan *et al.* 21.5 |
| **IO-BQAJ** (4) | **TS-A5B** | **YBOA** | 13.00 | -35.58 | Curran *et al.* 15.25 |
| **IO-BQDJ** (4) | **TS-D5B** | **YBOD** | 19.08 | -33.33 | Buda *et al.* 16.6 (15.5) |
| **IO-DQBJ** (4) | **TS-B5D** | **YBOD** | 12.98 | -18.88 | |
| **IO-DQDJ** (4) | **TS-D5D** | **YDOD** | 13.46 | -19.05 | |
| **IO-AQCJ** (5) | **TS-C5A** | **YCOA** | 6.19 | -35.71 | Wijaya *et al.* 11.5;13;14.8;[d] Chan *et al.* 16 |
| **IO-CQAJ** (5) | **TS-A5C** | **YCOA** | 9.33 | -39.16 | Curran *et al.* 7 ; Buda *et al.* 7 (9) |
| **IO-AQDJ** (6) | **TS-D5A** | **YAOD** | 7.06 | -42.21 | Chan *et al.* 17.9 |
| **IO-DQAJ** (6) | **TS-A5D** | **YAOD** | 6.37 | -42.71 | Curran *et al.* 1.8; Buda *et al.* 6 (1.95) |

[a] Hydroperoxy-alkyl radical, [b] Denotes as O-mediated cycles between two carbon centers, [c] Enthalpies, [d] Two, one and none $CH_3$- substituent groupsat adjacent to HOO• carbon atoms, respectively.

The same TS- numbering used above is used in the detailed PES of IO-CJ+$O_2$ for consistency. TSX5C stands for ring-closure and TSX7C for OH-transfer processes. A letter after numeration (here C-position) indicates initial peroxy-center, while the letter (X) before numbers shows reacting active site. For instance, TSA5C represents the TS5 (ring-closure) type transition state for hydroperoxy-alkyl radical IO-CQAJ proceeding via the loss of C-position OH and ring-closure (cyclization) at the A-radical site.

As seen from Tables 1 and 2, formation of both primary products is rather exothermic. *2,2,4,4*-tetramethyltetrahydrofuran (IO-YAOC, with Y-representing cycle and AOC – bonding between centers A and C mediated by an O-atom) is abundant in combustion as shown in isooctane experiments [6-10]. Hydroxyl-alkoxy radical (IO-AOHCOJ) is less stable. It rapidly decomposes via beta scission (barrier of 6.7 kcal $mol^{-1}$) to acetone and hydroxyl-neopentyl radical, which in turn can eliminate the important $^{\bullet}CH_2OH$ radical and form the abundant isobutene product, $(CH_3)_2C{=}CH_2$. Acetone is also an experimentally observed product [8].

Formation of hydroxyl-alkoxy intermediates, as seen from Table 2, faces varied barrier heights even in series with the same TS-ring size. Here the similarity of channels does not justify employment of similar parameters, which is in common application in current models. In addition, several other unique reaction channels, some with low energy barriers were identified and due to the restriction of length they will be presented in the elaborate version [17].

***Second Oxygenation Reactions.*** The role of low-temperature chain-branching, formation of a ketohydroperoxide + OH, which further forms an alkoxy radical and a second OH, is known to compete with dissociative ring-closure reactions in alkanes [13,14,18].

**Table 3. Enthalpy Barriers for Second Oxygenation Reactions Leading to Chain Branching Calculated at B3LYP/6-31G(d) Level**

| Reagent [a] | TS ring-size (Degeneracy) | Product [b] | $\Delta H^{\#}$, [c] kcal $mol^{-1}$ | Estimate [d] |
|---|---|---|---|---|
| **IO-AQAQJ** | 6 (9) | **IO-AQAQAJ** | 18.75 | 21.00 |
| **IO-AQBQJ** | 6 (9) | **IO-AQBQAJ** | 19.585 | 21.00 |
| **IO-AQCQJ** | 7 (9) | **IO-AQCQAJ** | *no access* | 19.35 |
| **IO-AQDQJ** | 8 (9) | **IO-AQDQAJ** | 23.05 | 22.55 |
| **IO-BQAQJ** [e] | 6 (2) | **IO-BQAQBJ** | 14.93 | 17.85 |
| **IO-BQCQJ** | 5 (2) | **IO-BQCQBJ** | 26.45 | 23.85 |
| **IO-BQDQJ** | 6 (2) | **IO-BQDQBJ** | 19.74 | 17.85 |
| **IO-DQAQJ** | 8 (6) | **IO-DQAQDJ** | 17.65 | 22.55 |
| **IO-DQBQJ** | 6 (6) | **IO-DQBQDJ** | 20.25 | 21.00 |
| **IO-DQCQJ** | 5 (6) | **IO-DQCQDJ** | 28.72 | 26.40 |
| **IO-DQDQJ** | 6 (6) | **IO-DQDQDJ** | 20.75 | 21.00 |

[a] Hydroperoxide-peroxy radicals undergoing intramolecular isomerization, [b] Di-hydroperoxide-alkyl radical intermediates (possibly in the form of vdW-complexes, *cf.* [18]), which initiate chain-branching by straightforward elimination of OH, [c] Enthalpy barrier, [d] Data extracted from Curran et al. model [10], where all barriers from first oxygenation step are consistently reduced by 3 kcal $mol^{-1}$ [e] C-position with only one tertiary hydrogen atom is skipped as no H-atom available at this stage attached to HOO-group.

The reactions include second oxygen association with the hydroperoxy alkyl radical and attack of the new peroxy center to an H-atom bonded to the carbon atom bearing HOO-group. The carbon radical containing hydroperoxide group then cleaves the weak RO—OH bond, eliminates OH and forms a strong carbonyl π-bond. Under chemical activation, the formed ketohydroperoxide can lose OH before stabilization, forming an alkoxy radical + a second OH. In alkanes these reactions are most favored for six member ring transition states [18]. How this does behaves in isooctane?

We have performed direct calculations for most relevant reactions for all four type H-atom positions to generate the second chemically activated peroxy radicals. The tertiary C-H bond is the weakest one and is expected to be cleaved easiest, as discussed above. However, after first oxygenation of this tertiary position no H-atom remains to be abstracted in the second step! Regular H-transfer (isomerization) though possible requires high barriers. If we consider the dominating IO-CQJ reactions in overall kinetics, then the absence of second oxygenation channel in this system could be a reason for the relative passivity or lower reactivity of isooctane at lower temperatures and pressures. For comparison, the barrier for isomerization of hydroperoxide-peroxy radical •OOROOH→ O=R'OOH+•OH in *n*-pentane (likely close to the one in *n*-heptane) calculated at CBS-QB3 level is only 15.7 kcal $mol^{-1}$ compared to the first isomerization barrier of 19.7 at the same level [18].

*We select all possible reactions involving adducts with H-atoms attached to OOH-group* (Table 3). In Curran's IO-mechanism [10] (and likely others) the barrier for a second H-transfer is reduced by 3 kcal $mol^{-1}$ compared to *n*-heptane, based on reasoning that a hydrogen atom to be abstracted is bound to a carbon atom which is bound to a hydroperoxy group should be more labile. However, the chemical activation component is not included, where the modeling results of Taatjes et al. [29,30] show that the chemical activation is needed to explain their low temperature radical profiles.

Results for isooctane are more complex and diverse (as detailed in [17]). For instance, there is significant steric hindrance (effectively no access) to the hydrogen at the HOO-bound carbon atom in the IO-AQCQJ radical intermediate (reaction IO-AQCJ+$O_2$ →IO-AQCQJ → IO-AQCQAJ). Hence, this seemingly analogous reaction to other known oxidation channels should be ruled out. In addition, our calculated data on isooctane show significant differences for many common reaction steps where current modeling uses estimates that are in good agreement with data for the reaction on less steric hindered systems.

Abstraction of hydrogen atom at C-position (the tertiary one) is easier when compared to other similar ring-strain isomerization processes. Though IO-DQCQJ is also sterically favored, the reaction IO-DQCJ+$O_2$ → IO-DQCQJ → IO-DQCQDJ requires somewhat higher barrier of 28.72 kcal $mol^{-1}$ (again for a 5-membered ring TS).

Energetically more feasible reaction is the attack of IO-BQAQJ radical center to the single remaining hydrogen bound to the B carbon atom bearing the HOO-group. This results in IO-BQAQBJ (barrier of 14.9 kcal $mol^{-1}$ *vs.* an averaged assigned literature value of 17.85 kcal $mol^{-1}$ [10]).

## 4. Concluding Remarks

A comprehensive mechanistic study is performed for the oxidation of isooctane based on direct calculations of PES involving *all possible* isooctyl radicals + $^3\Sigma^+_g(O_2)$ systems at DFT and higher levels of theory. To the best of our knowledge, this is the first attempt in literature to study the detailed PES and kinetic parameters using first principle methods for a real fuel component molecule as large as isooctane. This extensive investigation led to the identification of new channels for the formation of $H_2O$, $CH_2OH$ and olefins. It also showed that the similarity of channels does not justify employment of similar kinetic parameters, which is in common practice in most of the literature models such as Curran's and suggests that the rule of transferability of kinetic parameters needs to be refined. Along with the localization of TS and minima for variety of *a priori* and intuitively expected pathways, several new low-energy channels were explored (see, e.g., Fig 3). Such channels (IO-CQJ → TS-A1C → IO-CQAJ → TS-A5C → TMTHF + OH; IO-CQAJ → TS-A7C → IO-AOHCOJ → TS-A7Ca→…→ $CH_2OH$ + PR-2*M + Ac) seem essential to describe the products and key intermediates that have been observed experimentally [6-10]. The latter channel is believed to be exceedingly important due to the formation of •$CH_2OH$ and acetone.

The tertiary C-H bond is the weakest bond in isooctane and respective IO-CJ alkyl radical formation is believed to be straightforward in isooctane combustion at lower temperatures. A detailed PES is developed for the oxygenation and further activation reactions of IO-CJ, namely its association with oxygen to form IO-CQJ peroxy adduct, isomerization of IO-CQJ to IO-CQAJ, IO-CQBJ and IO-CQDJ hydroperoxy-alkyl radicals and their further reactions to variety of products.

We have characterized the two most relevant lowest energy pathways for the other peroxy radical reaction channels (involving primary IO-AQJ, IO-DQJ and secondary IO-BQJ radicals): dissociative ring-closure and OH-transfer from peroxy linkage to the radical center.

Calculations on this large branched alkane system show that the B3LYP/6-31G(d) hybrid DFT method with only one *d*-polarization function on second row elements, exhibits a reasonably good performance for reactions with C-C, C-O and O-O bond fission features important in chain branching at low and intermediate temperatures. It is reasonable to use this B3LYP functional for screening of PES's of these extended hydrocarbon systems despite some underestimate in dispersion interactions for H-transfer reactions. CBS-QB3 multilevel calculations appear to be well designed for characterizing energy gaps and activation barriers and results from such calculations will be published separately [17].

### Acknowledgments

We would like to thank Dr. John T. Farrell for helpful discussions. This research was supported by a Grant from EMREC.

### References

1. T. J. Wallington, E.W. Kaiserb, J.T. Farrell, Automotive fuels and internal combustion engines: a chemical perspective, *Chem. Soc. Rev*., 35 (2006) 335–347.

2. J.T. Farrell, N.P. Cernansky, F.L. Dryer, D.G. Friend, C.A. Hergart, Law C.K., R. McDavid, C.J. Mueller, H. Pitsch, *SAE Paper* 2007-01-0201.
3. J.M. Simmie, *Progress in Energy and Combust. Sci.* 29 (2003) 599.
4. H.-P.S. Shen, J. Vanderover, M.A. Oehlschlaeger, *Combust. Flame*, 155 (2008) 739 -755.
5. He X., Walton S.M., Zigler B.T., Wooldridge M.S., Atreya A. *Int. J. Chem. Kinet.* 39 (2007) 498.
6. A. Ciajolo, A. D'Anna, *Combust. Flame* 112 (1998) 617-622.
7. R. Minetti, M. Carlier, M. Ribaucour, E. Therssen, L.R. Sochet, *Proc. Combust. Inst.* 26 (1996) .
8. J.-S. Chen, T. A. Litzinger, H. J. Curran, Comb. Sci. and Tech.172 (2001)71; 156 (2000) 49.
9. F. Buda, R. Bounaceur, V. Warth, P.A. Glaude, R. Fournet, F. Battin-Leclerc, *Combust. Flame* 142 (2005) 170.
10. H.J. Curran, P. Gaffuri, W.J. Pitz, C.K. Westbrook, *Combust. Flame*, 129 (2002) 253.
11. F.F. Rust, *J. Amer. Chem. Soc.*, 79 (1957) 4000.
12. W.-T. Chan, H.O. Pritchard, I.P. Hamilton, *Phys. Chem. Chem. Phys.,* 1 (1999) 3715.
13. C.D. Wijaya, S. Raman, W.H. Green, Jr. *J. Phys. Chem.* 107(2003) 4908.
14. W. H. Green, Jr., C.D. Wijaya, P.E. Yelvington, S. Raman. *Mol. Phys.* 102 (2004) 371.
15. R. Asatryan, J.W. Bozzelli, *Phys. Chem. Chem. Phys.* 10 (2008)1769.
16. M. Mehl, H. J. Curran, W. J. Pitz, C. K. Westbrook, *Proc. Eur. Combust. Meet.* 2009.
17. R. Asatryan, S. Raman, P.A. Bielenberg, B. Peterson, J.W. Bozzelli, W. Weissman, Chain-Branching and Termination in the Low-Temperature Oxidation of Iso-Octyl Radicals, (2011) *to be submitted to J. Phys. Chem. A.*
18. R. Asatryan, J.W. Bozzelli *J. Phys. Chem. A* 114 (2010) 7693-7708.
19. J.W. Bozzelli, R. Asatryan, C.J. Montgomery, C. Sheng, Pressure Dependent Mechanism for H/O/C(1) Chemistry, *5th US Nat. Combust. Meet.* March 2007, San Diego.
20. C.J. Cramer, *Essentials of Computational Chemistry: Theories and Methods*, Wiley, New York, 2002.
21. Gaussian 03, Revision D.01, M. J. Frisch, et al. Gaussian, Inc., Pittsburgh PA, 2003.
22. J. Zheng, D.G. Truhlar, *Phys. Chem. Chem. Phys.,* 12 (2010) 7782.
23. J.A. Montgomery, Jr., M.J. Frish, J.W. Ochterski, G.A. Petersson, *J. Chem. Phys.* 110 (1999) 2822.
24. L. Zhu, J.W. Bozzelli, L.M. Kardos, *J. Phys. Chem.* 111 (2007) 6361.
25. R. Asatryan, J.W. Bozzelli, J.M. Simmie, *J. Phys. Chem. A,* 112 (2008) 3172-3185.
26. S. Sharma, S. Raman, W.H. Green, *J. Phys. Chem. A,* 114 (2010) 15689.
27. A.C. Davis, J.S. Francisco, *J. Phys. Chem. A,* 114 (2010) 11492-11505.
28. L.K. Huynh, H.-H. Carstensen, A.M. Dean, *J. Phys. Chem. A,* 114 (2010) 6594.
29. C. A. Taatjes, *J. Phys. Chem. A.,* 110 (2006) 4299.
30. J.D. DeSain, S. J. Klippenstein, J. A. Miller, C. A. Taatjes, *J. Phys. Chem. A*, 107 (2003) 4415.